Thermal Degradations of Chlorinated Natural Rubber from Latex and Chlorinated Natural Rubber from Solution

Ying Cai,[1] Si-Dong Li,[1,2] Cheng-Peng Li,[1] Pu-Wang Li,[2] Chen Wang,[1] Ming-Zhe Lv,[2] Kui Xu[2]

[1]*College of Science, Guangdong Ocean University, Zhanjiang 524088, People's Republic of China*
[2]*Agriculture Ministry Key Laboratory of Natural Rubber Processing, Agricultural Products Processing Research Institute, Chinese Academy of Tropical Agricultural Sciences, Zhanjiang 524001, People's Republic of China*

ABSTRACT: The thermal degradations of chlorinated natural rubbers from latex (CNR-L) and from solution (CNR-S) under nitrogen atmosphere were studied with thermogravimetric analysis (TGA). The thermal degradations of CNR-L and CNR-S are one-step reaction. The shapes of the thermogravimetric and derivative thermogravimetric curves are similar. The degradation temperatures of CNR-L and CNR-S increase linearly with the increment of heating rates. The heating rate hardly affects the thermal degradation rates of CNR-L and CNR-S at the various degradation stages. The thermal degradations of CNR-S and CNR-L are dehydrochlonation reactions. The reaction activation energy (E) of CNR, at the first stage, is around 100 kJ/mol. After that, E remains relatively steady (80–140 kJ/mol). At the last stage, E rises rapidly (130–270 kJ/mol). The variation tendency of frequency factor (A) is similar to that of E. As the initial degradation temperature T_0 of CNR-L is 10.9°C lower than that of CNR-S, the thermal stability of CNR-S is better than that of CNR-L, which may be caused by the difference of molecular structure between CNR-L and CNR-S, as FTIR results indicate that there are more —OH, —C=O and —COO— groups in the CNR-L molecular chains. © 2007 Wiley Periodicals, Inc. J Appl Polym Sci 106: 743–748, 2007

Key words: chlorinated natural rubber; thermal degradation; thermal stability; chlorinated process

INTRODUCTION

Chlorinated natural rubber (CNR) with flame-retardant and chemical resistant properties has been widely used in chemical- and heat-resistant paints, coatings, adhesives, and printing inks.[1–3] Traditionally, the CNR was prepared by dissolving the natural rubber in tetrachloromethane, and then chlorinating.[4,5] The advantages of the solution process include the easy control of the reaction, and fast chlorination. However, the solution process needs expensive equipment and high cost. Moreover, it produces a big amount of toxic solvent, which may be easily leaked and cause environmental hazards or be harmful to the health of workers. Recently, carbon tetrachloride has been banned in all industrial processes in advanced countries since it is suspected to damage the lay of atmospheric ozone.[6] Therefore, the solution process will be replaced by other processes sooner or later.

The production, structure and application of CNR have been widely studied.[7–14] Since the preparation of CNR from latex (CNR-L) was firstly reported in the 1930s,[15] scientists have tried many ways to prepare CNR-L, such as highly diluting the natural rubber latex, mixing with diatomite, drying to powder, adding base, vulcanizing, or adding stabilizer, as well as adding sodium hypochlorite and chloric acid. CNR with a chlorine content of 60% was prepared by Van Amerrongen[5] through adding stabilizer, then adding concentrated chloric acid or sulfuric acid to make the latex in a positive state and then passing the chlorine gas into the latex to carry out the chlorination reaction. However, the product possesses a poor solubility. The Rubber Research Institute of Sri Lanka have launched on preparing CNR from latex for years and have already prepared a stable CNR with a good solubility.[6] We overcame the coagulation of latex caused by the evolution of hydrochloric acid during chlorination, and prepared CNR directly from natural rubber latex.[16] The production cost of the latex process is US\$ 1.81/kg, while that of solution process is US\$ 3.01/kg. Obviously, the advantages of the latex process are not only the possibility to avoid the environmental pollution, but also the reduction of the production cost.

WILEY InterScience®
DISCOVER SOMETHING GREAT

The current study aims to investigate the effect of chlorinated process on thermal stability of CNR, and study the difference of thermal degradation between CNR from solution process (CNR-S) and CNR from latex process (CNR-L).

EXPERIMENTAL

Materials

CNR-S with a chlorine content of 63 wt %, was provided by China Guangzhou Chemical Industrial factory (Guangzhou, People's Republic of China). CNR-L, with a chlorine content of 63 wt %, was obtained from South China Chemical Industrial Company under South China Tropical Agricultural Product Processing Research Institute (Zhanjiang, People's Republic of China).

FTIR analysis

A Perkin–Elmer Spectrum-GX-1 infrared spectrometer was used to obtain FTIR data. FTIR spectra were recorded in the wave number range of 4000–400 cm^{-1} with a resolution of 4 cm^{-1}.

Thermogravimetric analysis

The thermogravimetric analysis (TGA) was performed on a Perkin–Elmer TGA-7 Thermal Gravimetric Analyzer. The mass of each sample was about $5.00 \sim 6.00$ mg. The carrier gas was nitrogen with a flow rate of 50 mL/min. The samples were heated from 50 to 600°C with the heating rates (B) of 10°C min^{-1}, 15°C min^{-1}, 20°C min^{-1}, 25°C min^{-1}, and 30°C min^{-1}, respectively.

Data processing

The reaction kinetic factors were obtained by the processing of TG data through the Friedman method.[17,18] In general, the thermal degradation reaction of a solid polymer can be simply show as: $B_{\text{solid}} \rightarrow C_{\text{solid}} + D_{\text{gas}}$ where B_{solid} is the starting material, C_{solid} and D_{gas} are the different products during the disappearance of B_{solid}. In thermogravimetric measurements, the degree of decomposition (conversion) can be calculated as follows:

$$X = \frac{W_0 - W_t}{W_0 - W_f} \qquad (1)$$

where X is degree of decomposition; W_t, W_0, and W_f are the actual, initial, and final mass of the sample, respectively. A typical model for a kinetic process can be expressed as:

$$\frac{dX}{dt} = kf(X) \qquad (2)$$

where dX/dt is the decomposition rate, $f(X)$, the function of X, depends on the particular decomposition mechanism. And k is the decomposition rate constant, which can be expressed by the Arrhenius equation:

$$k = A\exp\left(\frac{-E}{RT}\right) \qquad (3)$$

where A is the frequency factor (s^{-1}), E is the activation energy (J/mol), R is the gas constant (8.314 J mol^{-1} K^{-1}), and T is Kelvin temperature (K). Substituting the eq. (3) into eq. (2), we obtain

$$\frac{dX}{dt} = A\exp\left(\frac{-E}{RT}\right)f(X) \qquad (4)$$

If the temperature of a sample is changed by a constant value of B ($B = dT/dt$), the variation of the degree of decomposition can be analyzed as a function of temperature. Therefore, the reaction rate gives:

$$\frac{dX}{dT} = \frac{A}{B}\exp\left(\frac{-E}{RT}\right)f(X) \qquad (5)$$

The eqs.(4) and (5) are the basic equations for the kinetic calculation.

The Friedman method is a differential method, and it is based on eq.(4) whose logarithm is:

$$\ln\left(\frac{dX}{dt}\right) = \ln\left(B\frac{dX}{dT}\right) = \ln[Af(X)] - \frac{E}{RT} \qquad (6)$$

From this equation, it is easy to obtain values for E over a wide range of conversions by plotting $\ln(B(dX/dT))$ against $1/T$ at constant values of X. The slope of each line is $-E/R$ and the intercept is $\ln(Af(X))$.

RESULTS AND DISCUSSION

Thermal degradation of CNR-L and CNR-S

Figures 1–4 are the thermal degradation TG and DTG curves of CNR-L and CNR-S at five different heating rates in nitrogen. As can be seen, the TG curves are smooth and there is only one obvious turn on each TG curve and one corresponding peak on each DTG curve, indicating that the thermal degradation of CNR-L and CNR-S can be regarded as a one step reaction. It is also obvious that the TG and DTG curves shift toward the high temperature along with the increase of heating rate. The shapes of the
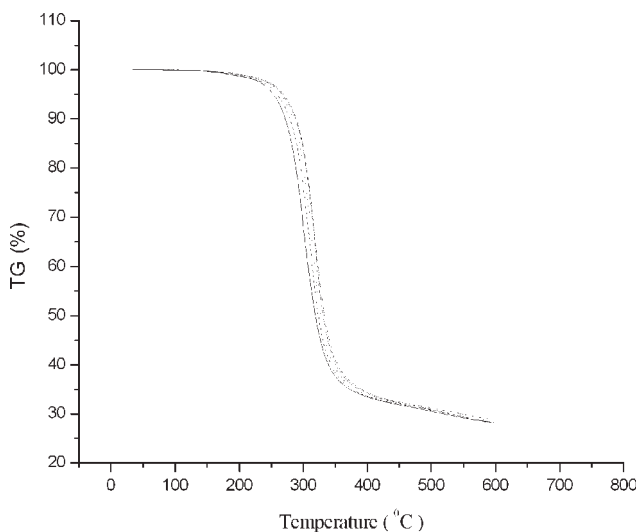
Figure 1 TG curves of thermal degradation of CNR-L. ((—)B = 10°C min^{-1}; (······)B = 15°C min^{-1}; (– – –)B = 20°C min^{-1}; (– ·– ·– ·)B = 25°C min^{-1}; (– ··– ··)B = 30°C min^{-1}).
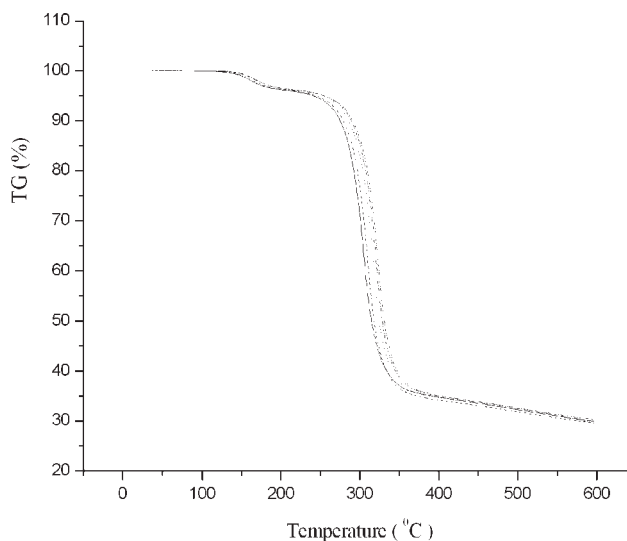
Figure 3 TG curves of thermal degradation of CNR-S ((—) B = 10°C min^{-1}; (······)B = 15°C min^{-1}; (– – –)B = 20°C min^{-1}; (– ·– ·– ·)B = 25°C min^{-1}; (– ··– ··)B = 30°C min^{-1}).

TG and DTG curves of both CNR-L and CNR-S at five different heating rates are very similar.

Relationship between B and the thermal degradation temperature

Figures 5 and 6 show the relationship between the heating rates (B) and thermal degradation temperatures of CNR-L and CNR-S in the thermal degradation. The initial degradation temperature (T_0) and the final degradation temperature (T_f) are obtained from the TG curves with the bi-tangent method, and T_p is the temperature of the maximum weight loss. It can be seen that the thermal degradation tempera-

tures increase linearly along with the increment of B. The relations between B and T_0, T_p and T_f of CNR-L are as follows:

$T_0 = 0.968B + 264.3°C$
$T_p = 0.860B + 293.3°C$
$T_f = 0.582B + 325.0°C$

And the relations between B and T_0, T_p, and T_f of CNR-S are as follows:

$T_0 = 0.894B + 275.2°C$
$T_p = 0.976B + 295.3°C$
$T_f = 0.816B + 314.7°C$

The peak width of DTG curve could be expressed as $T_f - T_0$. The peak width of CNR-L is $T_f - T_0 = -0.386B + 60.7$ and that of CNR-S is $T_f - T_0 = -0.078B + 39.5$.
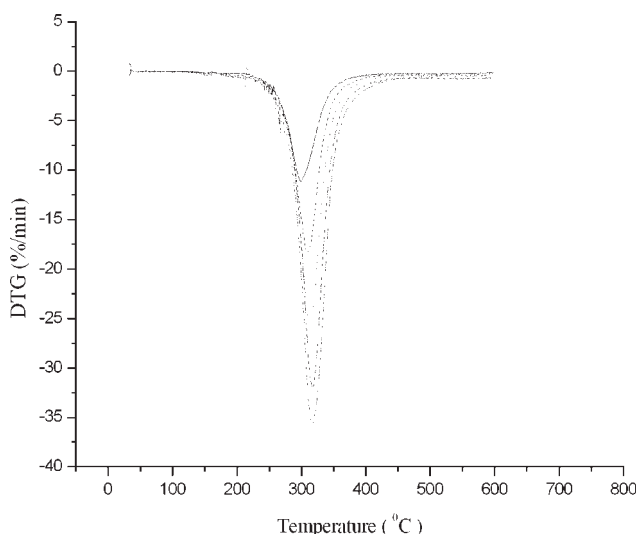

Figure 2 DTG curves of thermal degradation of CNR-L ((—)B = 10°C min^{-1}; (······)B = 15°C min^{-1}; (– – –)B = 20°C min^{-1}; (– ·– ·– ·)B = 25°C min^{-1}; (– ··– ··)B = 30°C min^{-1}).
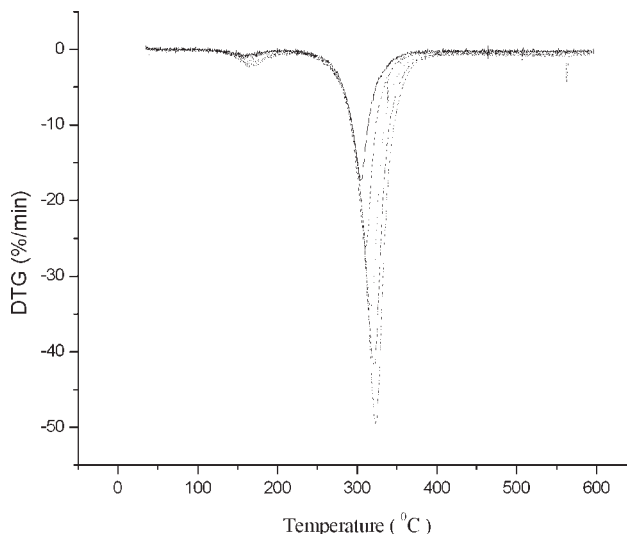
Figure 4 DTG curves of thermal degradation of CNR-S. ((—)B = 10°C min^{-1}; (······)B = 15°C min^{-1}; (– – –)B = 20°C min^{-1}; (– ·– ·– ·)B = 25°C min^{-1}; (– ··– ··)B = 30°C min^{-1}).
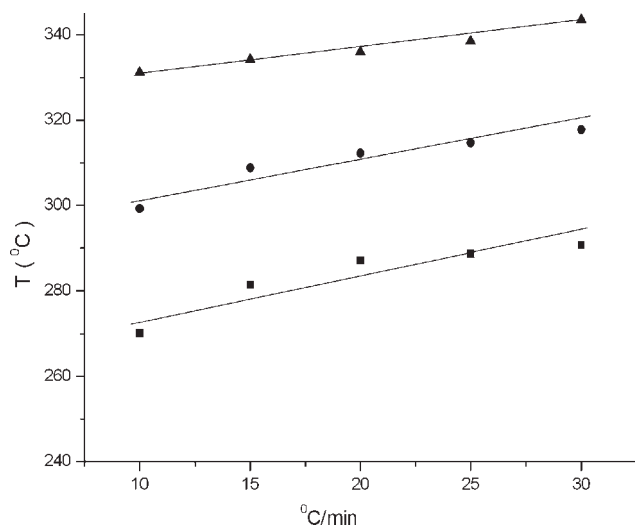
Figure 5 Relation between heating rate (B) and thermal degradation temperature of CNR-L (■: T_0 ●: T_p ▲: T_f).

It is obvious that the peak width of both CNR-S and CNR-L decreases with the increase of B.

The linear increase of the thermal degradation temperatures with the increment of B is caused by the heat hysteresis. Therefore, to eliminate the effect of heat hysteresis, the thermal degradation temperatures can be expressed as equilibrium temperatures (T^0), which is the thermal degradation temperatures when B approaches zero. The equilibrium thermal degradation temperatures of CNR-L in °C are expressed as follows:

$$T_0^0 = 264.3 \quad T_p^0 = 293.3 \quad T_f^0 = 325.0$$

The equilibrium thermal degradation temperatures of CNR-S are expressed as follows:

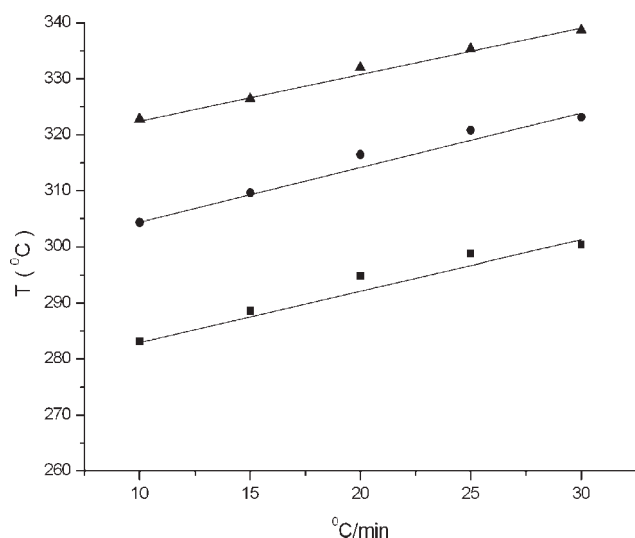$$T_0^0 = 275.2 \quad T_p^0 = 295.3 \quad T_f^0 = 314.7$$

Figure 6 Relation between heating rate (B) and thermal degradation temperature of CNR-S (■: T_0 ●: T_p ▲: T_f).

TABLE I
Relations Between Heating Rate (B) and Thermal Degradation Percentage of CNR-L

B °C/min	10	15	20	25	30	Mean
C_P (%)	32.6	34.7	33.9	35.2	34.6	34.2
C_f (%)	64.9	64.9	64.5	65.3	64.4	64.8

The degradation temperatures (T_0, T_p, and T_f) of CNR-L and CNR-S increase linearly along with heating rate. The values of T_p of CNR-L and CNR-S are very close, but the value of T_0 of CNR-L is 10.9°C lower than that of CNR-S, indicating that the thermal stability of CNR-L is not as good as that of CNR-S.

Effect of B on the thermal degradation rate

Tables I and II show the relationships between B and thermal degradation percentages (C_p and C_f) of CNR-L and CNR-S in nitrogen. The C_p and C_f are the thermal degradation percentages at T_p and T_f, respectively:

$$Cp = 100\% - \text{wt \% of residues}$$
$$Cf = 100\% - \text{wt \% of residues}$$

The results indicate that the C_p and C_f of CNR-L are not affected by heating rate, and their mean values are 34.2 wt % and 64.8 wt %, respectively. The un-decomposed residue account for about 35 wt % of the total mass, and the value of un-decomposed residue is stable in the temperature range (50–600°C) of the experiment.

The results in Table II indicate that the C_p of CNR-S increases slightly with the increasing of B and its average value is 38.3 wt %. The C_f of CNR-S is not affected by heating rate and its mean value is 64.9 wt %. The un-decomposed residue accounts for about 35 wt %, which is similar to that of CNR-L.

The C_p of CNR-S increase slightly with the increase of B, while the C_p of CNR-L is not affected by B and the mean value of C_p of CNR-L is 4.1% lower than that of CNR-S. The C_f of CNR-L and CNR-S is not affected by B and their mean value is 64.8% and 64.9%, respectively. The atomic weight of chlorine and hydrogen is 35.5 and 1.0, respectively. From the theoretic calculation, the ratio of the decreased weights of chlorine and hydrogen is 35.5:1.0 with the elimination of each molecule of

TABLE II
Relation Between Heating Rate (B) and Thermal Degradation Percentage of CNR-S

B °C/min	10	15	20	25	30	Mean
C_P (%)	36.5	37.7	38.5	38.9	39.9	38.3
C_f (%)	65.9	65.5	64.2	63.9	64.9	64.9

Figure 7 Relation between mass loss and activation Energy (E) and log A of CNR-L (E).
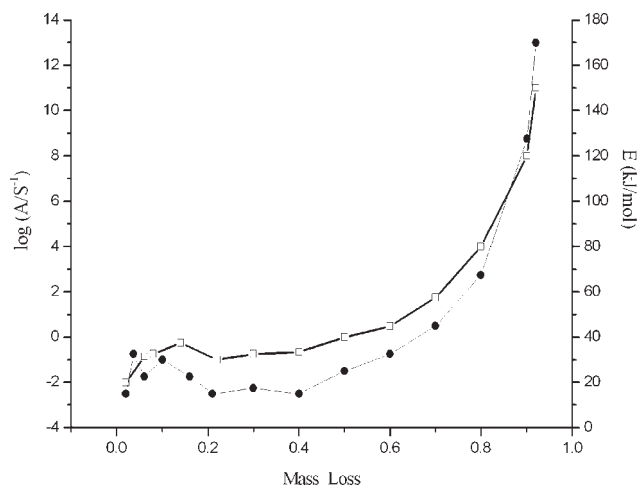

Figure 8 Relation between mass loss and activation Energy (E) and log A of CNR-S (●: E, □: log A).

HCl. In this experiment, the chlorine contents in CNR-L and CNR-S are 63%. When all the chlorine atoms were eliminated in the form of HCl, the hydrogen loss is 1.77% of the total weight of CNR. The total weight loss of chlorine and hydrogen is 64.77%, which equals to the C_f reasonably. It is obvious that the value of C_f from theoretic calculation is very close to that of test results.

Kinetics of thermal degradation of CNR-L and CNR-S

Figures 7 and 8 show the relation between fraction mass loss and Activation Energy (E) and frequency factor (A) of CNR-L. Figure 7 demonstrates that the activation energy (E) of CNR-L varies with mass loss during the thermal degradation process, which can be divided into three stages: 0–0.05, 0.10–0.60, and 0.70–1.0. At the first stage, the mean value of activation energy is about 100 kJ mol^{-1}, at the second stage, E remains relatively stable around 80–110 kJ mol^{-1}, while at the last stage, E rises rapidly (130–180 kJ mol^{-1}). The research performed by S.D.Li indicated that the thermal degradations of CNR-S and CNR-L are dehydrochlonation reaction.[19] The mean activation energies of the dehydrochlorination reaction of CNR-L is close to that of poly (vinylchloride) (96–126 kJ mol^{-1}).[20] The tendency of log$A$ is similar to that of E (Fig. 7).

Similar to CNR-L, the E of CNR-S can be divided into three stages: 0–0.05, 0.10–0.70, and 0.80–1.0 (Fig. 8). At the first stage, E is about 100 kJ mol^{-1}, the second stage, E remains relatively steady from 110 to 140 kJ mol^{-1}, and at the last stage, E rises rapidly from 180 kJ mol^{-1} to 270 kJ mol^{-1}. As the E of CNR-S is high than that of CNR-L, the thermal stability of CNR-S is better than that of CNR-L.
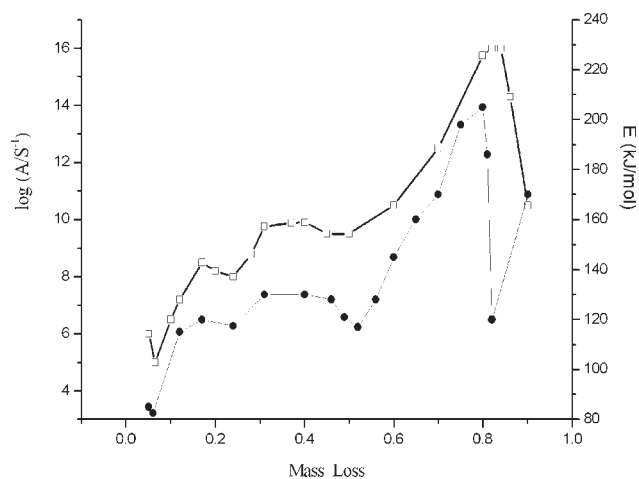
FTIR analysis

Figure 9 shows the FTIR spectra of CNR-L and CNR-S. In CNR-L, there are a wide absorbent band at 3504 cm^{-1} which is —OH stretching vibration in halogenated carboxyl group, absorption at 1738 cm^{-1} which is —C=O stretching vibration in halogenated carboxyl group, and absorption at 1622 cm^{-1} which is —COO— antisymmetric stretching vibration in carboxylate, while CNR-S just has some weak absorptions at same wave numbers.

—CH$_3$ antisymmetric stretching vibration is at about 2980 cm^{-1}, —CH$_3$ symmetric stratching vibration is at about 2856 cm^{-1}, —CH$_3$ symmetric deformation vibration is at about 1382 cm^{-1}, —CH$_2$ deformation vibration is at about 1441 cm^{-1}, —C—C— skeleton vibration is at about 1081 cm^{-1} and 1051 cm^{-1}, —CHCl stretching vibration could be at about 1430 cm^{-1} and 734 cm^{-1}, —CCl stretching vibration could be at about 1275 cm^{-1} and 788 cm^{-1} and 672 cm^{-1}, —CH$_2$Cl strtching vibration could be at about 937 cm^{-1}. Through FTIR analysis, it seems that the basic structure of CNR-L is similar to that of
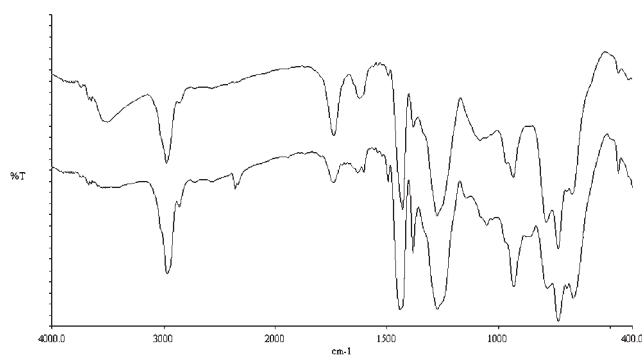

Figure 9 FTIR spectra of CNR-L and CNR-S. (the up spectrum is CNR-L; the down spectrum is CNR-S).

CNR-S, but the fine structures of both CNR are different. There are more amount carboxyl groups in CNR-L.

During preparation process of CNR-S, natural rubber polymer chains dissolved in CCl_4 were on the stretching state. In this way natural rubber molecules easily interact with Cl_2, and then the chlorinations are easier, in which the reaction temperature is lower and the reaction time is shorter. While in preparation of CNR-L, natural rubber molecules are compacted in the colloidal particle of water phase, so Cl_2 in water go through the surface of the colloidal particle first and then into the core of that, in which the chlorinations are difficult and reaction time is long. To speed up the chlorination, the reaction temperature should be lifted, but the oxidation of polymers would be difficult to avoid, so there are carboxyl compounds in the products. Cl_2 dissolved in water is easy to produce hypochlorous acid which has oxydation to the polymer, this is one of the causes to produce carboxyl groups in CNR-L.

CONCLUSIONS

The thermal degradations of CNR-L and CNR-S in nitrogen are one-step reaction of dehydrochlorination and the shapes of the TG and DTG curves are similar. The initial degradation temperature of CNR-S is 10.9°C higher than that of CNR-L, indicating that CNR-S should outperform CNR-L in thermal resistance. This is confirmed by the results of reaction activation energy, where the E of CNR-S is higher than that of CNR-L. The difference between CNR-S and CNR-L may be caused by the difference in molecular structure, i.e., there are more —OH, —C=O and —COO— groups exiting in the CNR-L molecular chains.

References

1. Fan, P. X. Chin Paint Ind 1996, 4, 14.
2. Huang, Y. X. Guangzhou Chem Ind 1989, 2, 8.
3. Wang, H. C. Chin Mod Chem Ind 1993, 8, 19.
4. Neethaand J. R. J. J Appl Polym Sci 1998, 68, 1185.
5. Van Amerongen, G. J. C.; Salomen, G. J Polym Sci 1950, 5, 629.
6. Seneviratne, W. M. G. Rubber Res Ins Sri-Lanka Annu Rev 1990, 68, 1.
7. Allirotand R.; Orsini, L. Rubber Chem Technol 1953, 26, 411.
8. Baxter, J. P. Rubber Chem Technol 1939, 12, 82.
9. Eskina, M. V.; Khachaturov, A. S.; Krentseland, L. B.; Litmanovich, A. D. Eur Polym Mater 1990, 26, 181.
10. Eskina, M. V.; Khachaturov, A. S.; Krentsel, L. B.; Yutudzhyanand, K. K.; Litmanovich, A. D. M V Vysokomol Soedin, Ser A 1988, 30, 142.
11. Koningsberger, C. Rubber Chem Technol 1953, 26, 406.
12. Krentsel, L. B.; Travin, S. O.; Litmanovichand, A. D.; Yutujan, K. K. Eur Polym Mater 1985, 21, 405.
13. Yang, D.; Li, S. D.; Fu, W. W.; Zhong, J. P.; Jia, D. M. J Appl Polym Sci 2003, 87, 199.
14. Yu, H. P.; Li, S. D.; Zhong, J P. J Appl Polym Sci 2006, 99, 1986.
15. Bloomfield, G. F. Rubber Chem Technol 1934, 7, 320.
16. Zhong, J. P.; Li, S. D.; Wei, Y. C.; Yu, H. J Appl Polym Sci 1999, 73, 2863.
17. Li, X. G.; Huang, M. R. Polym Degrad Stab 1999, 64, 81.
18. Yang, M. H. J Appl Polym Sci 2002, 86, 1540.
19. Li, S. D.; Peng, Z.; Yu. H. P.; Zhong, J. P.; Wei, Y. C. Chin Spectrosc Spectral Anal 1998, 4, 103.
20. Zhu, C. S. Chin Ageing Appl 1990, 2, 8.